Supporting Information

A Light-Up Fluorescence Resonance Energy Transfer Magnetic Aptamer-Sensor for Ultra-Sensitive Lung Cancer Exosome Detection

*Nanhang Zhu [1]; Guohao Li [1]; Juan Zhou [2]； Yujia Zhang [1]; Ke Kang [1]; Binwu Ying [2]; Qiangying Yi [1,] *; Yao Wu [1,] **

[1] National Engineering Research Center for Biomaterials, Sichuan University, Chengdu 610064, P. R. China

[2] Department of Laboratory Medicine, West China Hospital, Sichuan University, Chengdu, Sichuan 610041, P.R. China

Corresponding Author:

**E-mail: qyi@scu.edu.cn (Q.Y.).*

**E-mail: wuyao@scu.edu.cn (Y.W.).*

Tab. S1 Detailed information of aptamer sequences and modifications.

name	Sequence (5' to 3')	3' modification
Apt_{CD63}	CAC CCC ACC TCG CTC CCG TGA CAC TAA TGC TA	3`NH2 C6
$SH\text{-}DNA_{CD63}$	GAG CGA GGT GGG GTG TTT TTT TTT	3`SH C3
Apt_{EpCAM}	CAC TAC AGA GGT TGC GTC TGT CCC ACG TTG TCA TGG GGG GTT GGC CTG TTT	3`NH2 C6
$SH\text{-}DNA_{EpCAM}$	GCA ACC TCT GTA ATA TTT TTT TTT	3`SH C3

Tab. S2 Information of clinical samples.

Sample No.	Type	Gender	Age
1	Lung Cancer	Female	49
2	Lung Cancer	Female	69
3	Lung Cancer	Female	57
4	Lung Cancer	Female	49
5	Lung Cancer	Female	58
6	Lung Cancer	Female	64
7	Lung Cancer	Female	50
8	Breast Cancer	Female	48
9	Breast Cancer	Female	85
10	Breast Cancer	Female	67
11	Liver Cancer	Female	50
12	Thymic Carcinoma	Female	69
13	Health	Female	60
14	Health	Female	45
15	Health	Female	28

16	Health	Female	50
17	Health	Female	36
18	Health	Female	56

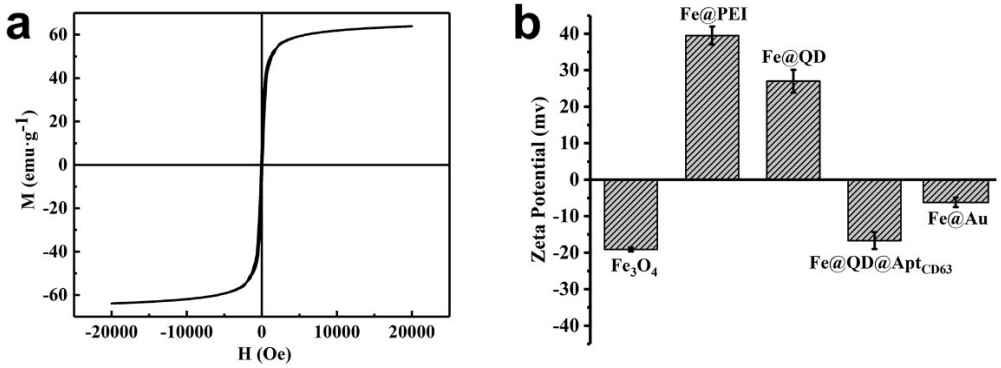

Fig. S1 (a) Magnetic hysteresis loop images of Fe nanoparticles. (b) Zeta potential of Fe_3O_4, Fe_3O_4@PEI, Fe_3O_4@QD, Fe_3O_4@QD@Apt_{CD63}, and Fe_3O_4@Au microparticles. All bars represent means ± SD (n = 3).

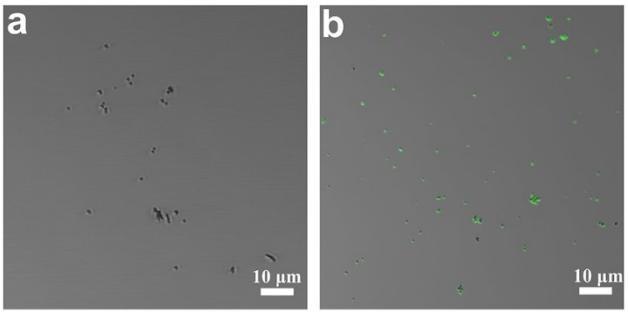

Fig. S2 CLSM images of (a) Fe_3O_4@PEI and (b) Fe_3O_4@PEI@QD.

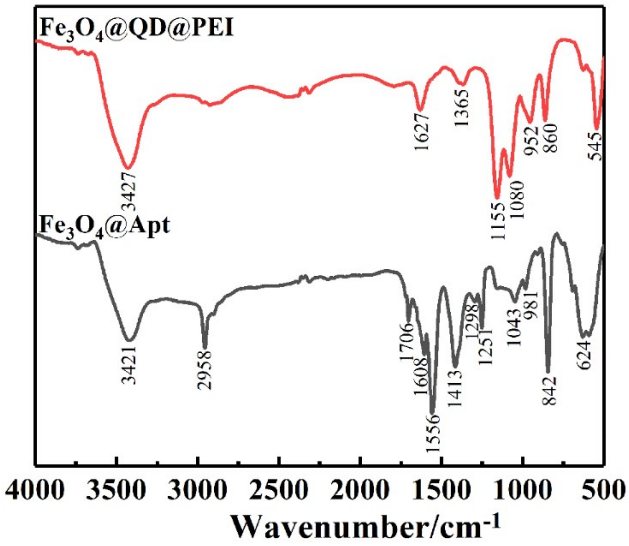

Fig. S3 The FT-IR spectra of Fe_3O_4@QD@PEI and Fe_3O_4@Apt.

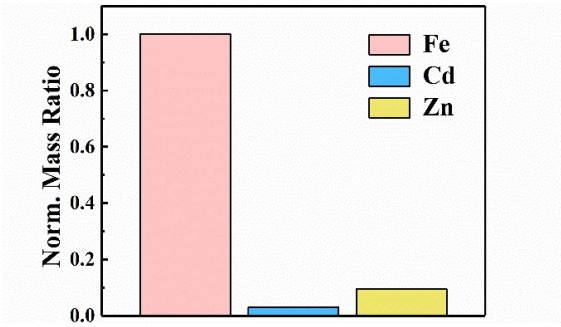

Fig. S4 ICP characterization calculation results of Fe_3O_4@QD.

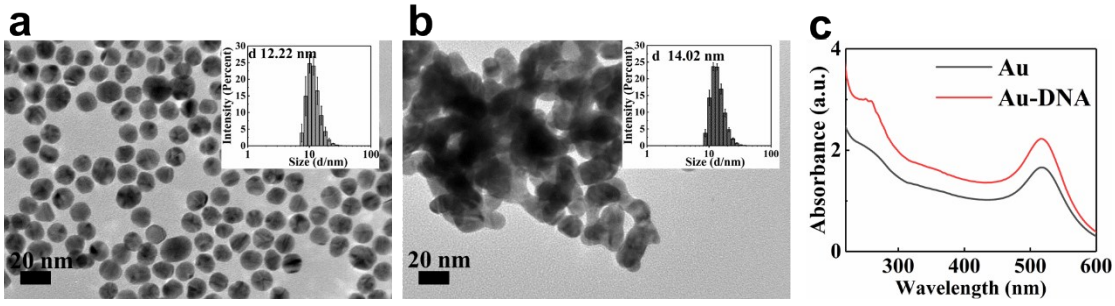

Fig. S5 TEM images of (a) Au nanoparticles and (b) Au-DNA nanoparticles. The insets illustrated their size distribution, respectively. (c) UV-vis absorbance spectra of Au and Au-DNA nanoparticles.

Recovery Efficiency

To study on recovery efficiency of the magnetic nanoparticle-exosome complexes, UV-vis absorbance at 641 nm of the supernatant after magnetic separation for a certain period of time was measured, and then referred to the standard curves established by UV-vis absorbance of the Fe_3O_4@Au@exo suspensions with known concentrations (8-500 ug/mL) to calculate amount of recovered materials. Finally, a scatter line graph of the recovery efficiency versus time was drawn.

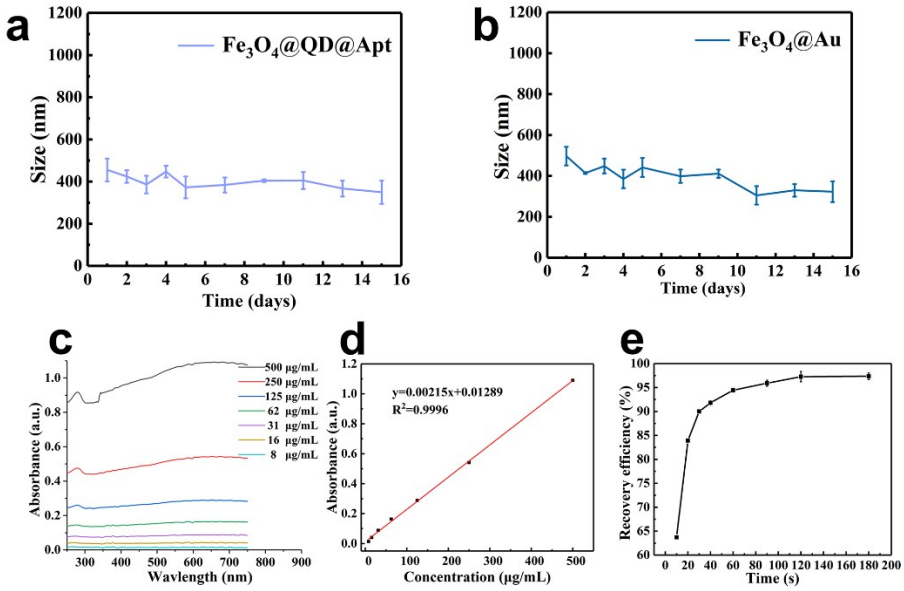

Fig. S6 Storage stability curve of (a) Fe_3O_4@QD@Apt and (b) Fe_3O_4@Au respectively. (c) UV-vis absorbance spectra and linear relationship (d) of different concentrations of Fe_3O_4@Au@exo. (e) Recovery efficiency of Fe_3O_4@Au@exo. The error bars refer to the standard deviations across three repeated measurements.

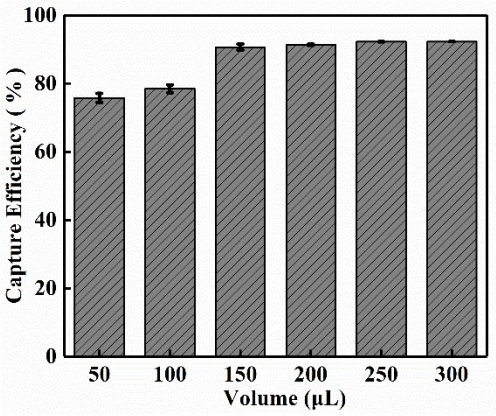

Fig. S7 Exosomes capture efficiencies of Fe_3O_4@Au at different volume. The error bars refer to the standard deviations across three repeated measurements.

Tab. S3 The fluorescence intensity recovery experimental results in model samples.

Exosomes Concentration (particles / mL)	Peak value at 520 nm (CPS / MicroAmps) (repeated 3 times)			Average (CPS / MicroAmps)	STDEV	Fluorescence Recovery (CPS / MicroAmps)	RSD
	1	2	3				
5×10^9	439227	440595	422578	434133	10031	206675	2.31%
5×10^8	386330	400300	403298	396643	9056	169185	2.28%
5×10^7	367014	362444	351006	360155	8246	132697	2.29%
5×10^6	332136	319697	336023	329285	8528	101827	2.59%
5×10^5	290281	293913	299829	294674	4819	67216	1.64%
5×10^4	272213	268492	256675	265793	8113	38335	3.05%
5×10^3	248835	249280	241705	246607	4251	19149	1.72%
5×10^2	234811	230621	238943	234792	4161	7334	1.77%

** STDEV: Standard Deviation, RSD: relative standard deviation.*

Tab. S4 The fluorescence intensity recovery experimental results in real samples with (a) CD63-containing and (b) EpCAM-containing system.

(a)

Samples	Peak value at 520 nm (CPS / MicroAmps) (repeated 3 times) 1	2	3	Average (CPS / MicroAmps)	STDEV	Fluorescence Recovery (CPS / MicroAmps)	**RSD**
Health 1	327131	337560	342921	335871	8029	108413	2.39%
Health 2	299607	311784	310669	307353	6732	79895	2.19%
Health 3	337893	337347	331498	335579	3545	108121	1.06%
Health 4	291140	285736	285021	287299	3346	59841	1.16%
Health 5	288137	284082	271913	281377	8443	53919	3.00%
Health 6	320940	315436	306140	314172	7481	86714	2.38%
Lung cancer 1	311010	303241	302278	305510	4788	78052	1.57%
Lung cancer 2	330259	324670	323575	326168	3585	98710	1.10%
Lung cancer 3	307702	309670	304837	307403	2430	79945	0.79%
Lung cancer 4	320287	328636	322963	323962	4263	96504	1.32%
Lung cancer 5	328145	320149	323122	323805	4042	96347	1.25%
Lung cancer 6	336416	333992	333825	334744	1450	107286	0.43%
Other cancer 1	324527	319364	309207	317699	7794	90241	2.45%
Other cancer 2	301625	289391	287168	292728	7785	65270	2.66%
Other cancer 3	342056	332194	328512	334254	7003	106796	2.10%
Other cancer 4	355272	343594	342304	347057	7144	119599	2.06%
Other cancer 5	349279	336782	337171	341077	7106	113619	2.08%
Other cancer 6	326779	325111	307045	319645	10944	92187	3.42%

(b)

Samples	Peak value at 520 nm (CPS / MicroAmps) (repeated 3 times) 1	2	3	Average (CPS / MicroAmps)	STDEV	Fluorescence Recovery (CPS / MicroAmps)	**RSD**
Health 1	383825	389428	380669	384641	4436	65510	1.15%
Health 2	360995	371965	370507	367822	5957	48691	1.62%
Health 3	358263	378619	381073	372652	12521	53521	3.36%

Health 4	376517	386046	379592	380718	4863	61587	1.28%
Health 5	349733	364844	357266	357281	7556	38150	2.11%
Health 6	376517	393258	391173	386983	9123	67852	2.36%
Lung cancer 1	349733	357385	343826	350315	6798	31184	1.94%
Lung cancer 2	405763	422523	419249	415845	8883	96714	2.14%
Lung cancer 3	439256	453013	448893	447054	7060	127923	1.58%
Lung cancer 4	413960	431233	428316	424503	9246	105372	2.18%
Lung cancer 5	435304	458357	459007	450889	13501	131758	2.99%
Lung cancer 6	435157	450439	447963	444520	8202	125389	1.85%
Other cancer 1	452828	474058	471586	466157	11610	147026	2.49%
Other cancer 2	419407	437118	439593	432039	11010	112908	2.55%
Other cancer 3	444349	461405	454582	453445	8585	134314	1.89%
Other cancer 4	438492	454341	450779	447871	8315	128740	1.86%
Other cancer 5	444349	462352	461728	456143	10219	137012	2.24%
Other cancer 6	482645	496621	495349	491538	7728	172407	1.57%

** STDEV: Standard Deviation, RSD: Relative Standard Deviation.*

Tab. S5 Comparison of different sensor for exosome detection.

Sensor Type	Detection unit	Recognition probe	Cell lines	Human samples	LOD (particles/mL)	Ref.
Uv - vis	s-SWCNTs	CD63 aptamer	MCF-7 MCF-10A	--	5.2×10^{8}	[1]
Uv - vis	ZnO nanowires	Anti-CD63, anti-CD9 antibody	MCF-7	--	2.2×10^{7}	[2]
Uv - vis	G-quadruplex	MUC1 aptamer	MCF-7	Serum	3.94×10^{5}	[3]
Uv - vis	Magnetic beads	Anti-LMP1, anti-EGFR antibody	NPC	Plasma	100	[4]
Electrochemical	Au-NPFe_2O_3NC	Anti-CD63 antibody	BeWo	--	1000	[5]
Electrochemical	Glassy carbon electrode	CD63 aptamer	MCF-7	Serum	9.6×10^{4}	[6]
Electrochemical	Anti-CD63/IMBs	Anti-CD63 antibody	HepG2 MCF-10A	--	1.72×10^{4}	[7]

Electrochemical	Carbon electrode	Anti-CD63, anti-CD9, anti-HER2 antibody	BT-474 SW-48	Serum	1.0×10^5	[8]
SERS	AuNS@4-MBA@Au and Magnetic beads	Anti-CD9 antibody	HepG2	Serum	2.7×10^4	[9]
SERS	SERS tags and glass slide	Anti-CD9, anti-CD63, anti-GPC1, anti-MIF antibody	PANC-01 HPDE6-C7	Serum	5×10^5	[10]
SERS	Magnetic beads	CD63, PSMA aptamer	SKBR3 T84 LNCaP	Blood	3.2×10^4	[11]
SERS	SERS tags and Fe3O4@TiO2	Anti-PD-L1 antibody	A549 BEAS-2B	Serum	1000	[12]
SPR	Dual AuNP	CD63 aptamer	MCF-7	--	5000	[13]
RRS	Nanoporous membrane and AuNC AuNC	Anti-CD63, anti-CD81 antibody	No	Urine	1000	[14]
Fluorescence	BRCA amplification	MUC1 aptamer	SGC7901	Plasma	4.27×10^4	[15]
Fluorescence	Magnetic beads	CD63, EpCAM aptamer	A549	Serum	428	this work

[a]SERS, surface-enhanced raman scattering; [b]SPR, surface plasmon resonance; [c]RRS, Resonance Rayleigh scattering.

"--" means not mentioned.

Reference

1. Y. Xia, M. Liu, L. Wang, A. Yan, W. He, M. Chen, J. Lan, J. Xu, L. Guan and J. Chen, *Biosensors & Bioelectronics*, 2017, **92**, 8-15.
2. Z. Chen, S.-B. Cheng, P. Cao, Q.-F. Qiu, Y. Chen, M. Xie, Y. Xu and W.-H. Huang, *Biosensors & Bioelectronics*, 2018, **122**, 211-216.
3. Y. Zhou, H. Xu, H. Wang and B.-C. Ye, *Analyst*, 2020, **145**, 107-114.
4. W. Liu, J. Li, Y. Wu, S. Xing, Y. Lai and G. Zhang, *Biosensors and Bioelectronics*, 2018, **102**, 204-210.
5. K. Boriachek, M. K. Masud, C. Palma, P. Hoang-Phuong, Y. Yamauchi, M. S. A. Hossain, N. Nam-Trung, C. Salomon and M. J. A. Shiddiky, *Analytical Chemistry*, 2019, **91**, 3827-3834.
6. Y. An, T. Jin, Y. Zhu, F. Zhang and P. He, *Biosensors & Bioelectronics*, 2019, **142**, 111503.
7. Y. Cao, L. Li, B. Han, Y. Wang and J. Zhao, *Biosensors & Bioelectronics*, 2019, **141**, 111397.
8. K. Boriachek, M. N. Islam, V. Gopalan, A. K. Lam, N.-T. Nguyen and M. J. Shiddiky, *Analyst*, 2017, **142**, 2211-2219.
9. Y.-F. Tian, C.-F. Ning, F. He, B.-C. Yin and B.-C. Ye, *Analyst*, 2018, **143**, 4915-4922.
10. Y. Bai, B. Zhang, L. Chen, Z. Lin, X. Zhang, D. Ge, W. Shi and Y. Sun, *Nanoscale Research Letters*, 2018, **13**, 287.
11. Z. Wang, S. Zong, Y. Wang, N. Li, L. Li, J. Lu, Z. Wang, B. Chen and Y. Cui, *Nanoscale*, 2018, **10**, 9053-9062.
12. Y. Pang, J. Shi, X. Yang, C. Wang, Z. Sun and R. Xiao, *Biosensors and Bioelectronics*, 2020, **148**, 111800.
13. Q. Wang, L. Zou, X. Yang, X. Liu, W. Nie, Y. Zheng, Q. Cheng and K. Wang, *Biosensors and Bioelectronics*, 2019, **135**, 129-136.
14. Q. Yang, L. Cheng, L. Hu, D. Lou, T. Zhang, J. Li, Q. Zhu and F. Liu, *Biosensors & Bioelectronics*, 2020, **163**, 11290.
15. R. Huang, L. He, S. Li, H. Liu, L. Jin, Z. Chen, Y. Zhao, Z. Li, Y. Deng and N. He, *Nanoscale*, 2020, **12**, 2445-2451.